Kinetics and luminescence of the excitations of a nonequilibrium polariton condensate

T. D. Doan,[1] D. B. Tran Thoai ●,[1] and H. Haug[2,*]

[1]*Ho Chi Minh City Institute of Physics, Vietnam Academy of Science and Technology, 1 Mac Dinh Chi, 70072 HoChi Minh City, Vietnam*
[2]*Institut für Theoretische Physik, Goethe-Universität Frankfurt, Max-von-Laue-Straße 1, D-60438 Frankfurt am Main, Germany*

We extend the description of the nonequilibrium Gross-Pitaevskii equation for microcavity polaritons by including not only the kinetics of the nonresonantly pumped exciton reservoir but also that of the collective excitations—called bogolons—above the condensate. Quasiequilibrium Hartree-Fock-Bogoliubov-Popov self-energies are used to describe the condensate and the bogolons. With nonequilibrium Green functions, the quantum Boltzmann equation of the bogolons in a frame moving with the condensate, together with the coupled Gross-Pitaevskii equation can be derived. The resulting scattering rates contain vertex corrections in form of symmetrized products of the *u* and *v* pairing functions of all involved scattering states. Corresponding results have been derived for ultracold atoms by A. Griffin, T. Nikuni, and E. Zaremba [*Bose-Condensed Gases at Finite Temperatures*, 1st ed. (Cambridge University Press, Cambridge, New York, 2009)] Furthermore, we show that the results of the quantum kinetics also determine the luminescence spectrum including the ghost branch. The kinetics is solved numerically, the resulting condensate, the bogolon distribution, and the luminescence are calculated temporally and spatially resolved after the switch-on of a *cw* nonresonant pump beam with a Gaussian profile. It is studied in detail to which extent the bogolons approach a local thermal equilibrium.

I. INTRODUCTION

A great simplification of the description of a spatially and temporally varying polariton condensate was obtained by cutting the polariton spectrum into a photonlike part in which the condensation takes place and into a higher-lying uncondensed excitonlike reservoir [1]. In other words, one disregards details of the polariton spectrum and treats instead essentially the two branches of the photons and the excitons which constitute the polariton as separate entities. The polariton condensate in the photonlike branch is described by a Gross-Pitaevskii equation [2] as for cold atoms [3], while the nonresonantly excited excitons act as a reservoir which is usually described by a rate equation for the excitons [1]. We have generalized the description of the reservoir by a quantum kinetic derivation which results in a quantum Boltzmann equation for the exciton reservoir [4] and self-consistently calculated transition probabilities between reservoir (r) and condensate (c). As the dominant gain mechanism, the particle-particle scattering has been treated. However, a single scattering event is in general not sufficient to bring a polariton from the reservoir down into the condensate. A more realistic picture evolves if the scattering from the reservoir into excited states above the condensate is taken into account. In other words, the kinetics can be made more complete by including the Bogoliubov excitations of the condensate, called bogolons (b). The hierarchy of the excitation kinetics is then

$$r \rightarrow b \rightarrow c . \tag{1}$$

We treat the case of a relatively large negative detung in order to open up a sufficiently large enrgy range for the considered bogoln relaxation kinetics. For a CdTe microcavity with a Rabi splitting of 28 meV a detuning of −6 meV is assumed which results in an energy depth of the photonlike branch below the resevoir of 13 meV.

For ultracold atoms, Griffin *et al.* [5] treated the Gross-Pitaevskii equation coupled to a Boltzmann equation for the Hartree-Fock-Popov excitations of the condensate. Extending this work Griffin *et al.* [6] formulated the kinetics of the excitations above the condensate in the Bogoliubov-Popov spectrum. Independently, Gust and Reichl [7] also derived the bogolon kinetics with the same results using a combination of Liouville equation techniques and the pairing theory.

Assuming an adiabatic approximation the gap-free Bogoliubov-Popov spectrum with a slowly varying space- and time-dependent condensate density $n_0(R, T)$ is given by [8]

$$e_{b,k} = \hbar\omega_{b,k} = \sqrt{e_k^2 + 2g_0 n_0(R, T)e_k} , \tag{2}$$

where g_0 is the *p-p* interaction matrix element, and $e_k = \hbar^2 k^2/2m$ is the free particle energy. In contrast to the Bogoliubov theory, which is only valid if $n_0/n \simeq 1$, the Popov theory remains at least qualitatively correct for variations of n_0 from 0 to n. The slowly varying condensate density is obtained from the solution of the Gross-Pitaevskii equation for the condensate wave function. The nonequilibrium modifications of the Bogoliubov spectrum at small k-values due to the coupling to the reservoir [1,9] can also be build in this spectrum as discussed further in Appendix B.

The bogolon distribution $n_{b,k}(R, T)$ which is a function of the 2D momentum k is in general also a slowly varying
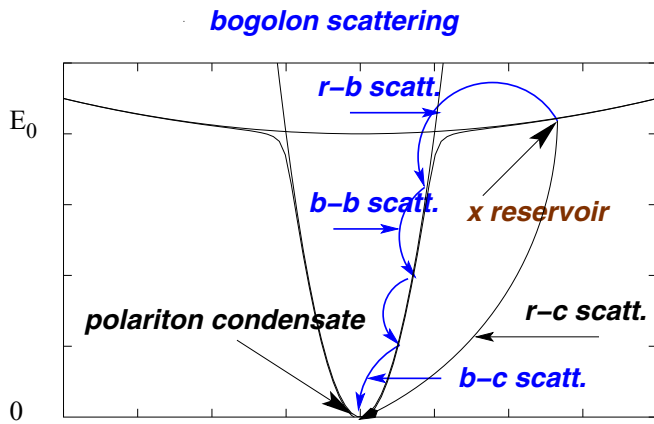
*haug@itp.uni-frankfurt.de

FIG. 1. Extended relaxation scheme by including the bogolon scattering. The reshaping of the bogolon spectrum by the condensation is not shown.

function in the 2D space coordinate R and the time T. To include the variation of the bogolon distribution with R, T is important, because often structured beams are used to pump the coupled reservoir. Besides, the coupled condensate often shows rather nontrivial structure formation. Thus the bogolon distribution should be described by a quantum Boltzmann equation. Considering only particle-particle scattering, which is dominant in a condensed system as shown by Roumpos *et al.* [10], the quantum Boltzmann equation of the collective excitations has the form

$$\frac{\partial n_{b,k}}{\partial T} + \nabla_k(e_k + U(R,T))\nabla_R n_{b,k}$$
$$- \nabla_R(e_k + U(R,T))\nabla_k n_{b,k} = \left.\frac{dn_{b,k}}{dT}\right|_{\text{scatt}}. \quad (3)$$

$U(R,T)$ is an external potential and the scattering rates are according to Fig. 1

$$\left.\frac{dn_{b,k}}{dT}\right|_{\text{scatt}} = -\gamma_k n_{b,k} + \left.\frac{dn_{b,k}}{dT}\right|_{r-b} + \left.\frac{dn_{b,k}}{dT}\right|_{b-b} + \left.\frac{dn_{b,k}}{dT}\right|_{b-c}. \quad (4)$$

Here the radiative decay is included by the first term. The damping coefficient $\gamma_k = \gamma_c|C_k|^2$ is the escape probability per unit time for a bogolon to leave the cavity as a photon. C_k is the photon Hopfield coefficient and γ_c is the cavity loss constant. Modifications of the Boltzmann equation due to a moving condensate will be discussed later. The derivation of the bogolon scattering rates needs a combination of the pairing theory with the standard quantum kinetic theory for a self-consistent derivation of the scattering rates from the Kadanoff-Baym equation for the kinetic component of the nonequilibrium Keldysh-Green functions.

A corresponding quantum Boltzmann equation for the uncondensed reservoir excitons coupled to the condensate has already been derived by us previously [4], which is commonly simplified to a rate equation with the assumption of thermal equilibrium in the reservoir.

As already derived for ultracold atoms the resulting bogolon scattering rates have the usual form of Fermi's golden rule with the initial and final states bogolon distribution functions and the self-consistently determined Bogoliubov-Popov energies. However, the bogolon scattering matrix elements

have vertex corrections in terms of a symmetrized products of the u_k, v_k pairing functions of all involved states. We use for our studies these vertex corrections in the particularly transparent form of Gust and Reichl [7].

An alternative approach would be to start from the coupled exciton-photon equations. Maybe this formulation would allow to include more polariton features, but it would lack the advantage to include directly the well-developed kinetics of excitations in atomic systems into our treatment. Therefore, we did not pursue this approach.

Compared to the earlier applied semiclassical rate equations for the polariton condensation kinetics [11–13] there are two major advances. Firstly, we include now the quantum statistically modified spectrum above the condensate. The separation of the polariton spectrum in a photonlike part and an exciton reservoir allows to include the modified Bogoliubov spectrum analytically.

Secondly, we allow in contrast to earlier studies of the condensation kinetics by rate equations in terms of a semiclassical Boltzmann kinetics slow spatial variations of the condensate, the population of the bogolons, and the nondegenerate population of the reservoir. The spatial variations make the physics of condensed systems much richer, they allow to treat the dynamics of topological defects such as vortices and solitons as well as spontaneous structure formation [4,14]. Including the excitations above the condensate is an improvement compared to the nonequilibrium Gross-Pitaevskii equation with condensate and reservoir only [1,4]. The price for this improvement is naturally an increase in the complexity of the description. However, the recent observations [15,16] of the luminescence of the bogolons need such a theory for their description.

Our approach also differs from more recent attempts to include the bogolons in terms of a stochastic Gross-Pitaevskii equation in which the scattering rates between the condensate and the excited states characterize the second moments of the fluctuations [17,18]. A complete inclusion of the whole bogolon kinetics is not possible in such an approach. Naturally each treatment of the condensation kinetics in terms of the homogeneous Gross-Pitaevskii equation needs some form of kinetic symmetry breaking. We include it by using stochastic infinitesimal initial conditions, but we do not use fluctuations which are present during the whole evolution of the condensate.

In the following, we discuss briefly how the quantum Boltzmann equation for the bogolons can be derived from the Kadanoff-Baym equation for the kinetic component of the Keldysh nonequilibrium Green function. We list the resulting scattering rates and discuss why the Boltzmann equation has to be formulated in a frame moving with the condensate. This is particularly important for nonresonantly excited microcavity polaritons in which often complex structure formation takes place by a flowing condensate. The coupled nonequilibrium Gross-Pitaevskii equation for the condensate wave function will be listed with the bogolon-condensate scattering rate. We show that the luminescence spectrum is given also by the kinetic component of the bogolon Green function. We solve the resulting bogolon and condensate kinetics for a CdTe-type polariton microcavity excited nonresonantly with a continuously switched-on stationary Gaussian pulse. A richly structured bogolon distribution is obtained. The approach of

the bogolons to a local thermal equilibrium is examined in detail by fitting the calculated bogolon distribution at various space and time points with a local equilibrium distribution. The resulting luminescence spectra including their ghost branches are determined.

II. THE QUANTUM BOLTZMANN EQUATION FOR BOGOLONS

For the derivation of the quantum Boltzmann equation for the bogolons from the Kadanoff-Baym equation for the kinetic component $G^<(t, t')$ of the Keldysh nonequilibrium Green functions, one can follow the common quantum kinetic theory [19]. The essential point is that for the bogolons the generalized Kadanoff-Baym ansatz has to be extended to a two-by-two matrix form. By these means, the anomalous spectral properties of the bogolons are taken approximately into account. Because we want to get a kinetic description for the build-up of the polariton condensate with increasing nonresonant pumping via the exciton reservoir to a fully developed polariton condensate, we have to use an extension of the Bogoliubov theory which holds only, if the majority of the particles are already in the condensate. Popov [8] showed that a gap-free spectrum can be obtained if also the contributions of the noncondensate are taken into account in the Hartree-Fock approximation of the self-energies of the condensate and the excitations. This formulation allows describing at least qualitatively the condensate threshold region in contrast to the simple Bogoliubov description. This approach has been studied in detail for condensed atomic systems by Griffin *et al.* [6].

Writing the boson field operator as

$$\Psi(\vec{r}, t) = \Psi_0(\vec{r}, t) + \psi(\vec{r}, t), \quad (5)$$

where $\Psi_0(\vec{r}, t) = \langle \Psi(\vec{r}, t) \rangle$ is the condensate wave function and $\psi(\vec{r}, t)$ the operator of the uncondensed particles. Because we have to take anomalous correlations into account, we use the convenient spinor notation with the components

$$\begin{pmatrix} \psi(\vec{r}, t)_1 \\ \psi(\vec{r}, t)_2 \end{pmatrix} = \begin{pmatrix} \psi(\vec{r}, t) \\ \psi^\dagger(\vec{r}, t) \end{pmatrix}. \quad (6)$$

The nonequilibrium Green functions (GF) become 2×2 matrices

$$G(\vec{r}, t; \vec{r}', t')_{ij} = -i \langle T_c \psi(\vec{r}, t)_i \psi^\dagger(\vec{r}', t')_j \rangle, \quad (7)$$

where T_c is the time ordering on the Keldysh contour. A similar matrix extension has been used for the quantum kinetics of a two-band semiconductor [19]. According to the four possibilities of the order of the two-time arguments on the forward and backward running parts of the contour, we get four types of nonequilibrium GF. We choose the following GF's:

$$G^<(\vec{r}, t; \vec{r}', t')_{ij} = -i \langle \psi^\dagger(\vec{r}', t')_j \psi(\vec{r}, t)_i \rangle. \quad (8)$$

For $i = j = 1$ this lesser function $G^<(\vec{r}', t'; \vec{r}, t)_{11}$ is the particle correlation function in space and time. Its diagonal limit $\vec{r}' = \vec{r}$ and $t' = t$ yields simply the time evolution of the particle density. Its off-diagonal behavior describes the long-range spatial and temporal decay of correlations in the excitation field. The function $G^<(\vec{r}', t'; \vec{r}, t)_{11}$ determines not only the

nonequilibrium quantum kinetics of the polaritons, but it also describes the luminescence from the excitations above the polariton condensate in the microcavity.

In addition to these kinetic GF's, two spectral Beliaev GF's:

$$G^r(t, t')_{ij} = -i\Theta(t - t') \langle [\psi(t)_i, \psi^\dagger(t')_j] \rangle, \quad (9)$$

which is the retarded GF. The advanced GF can be obtained with the relation $G^a(t, t')_{ij}^\star = G^r(t', t)_{ji}$, thus one can choose $G^<(t, t')_{ij}$ and $G^r(t, t')_{ij}$ as the basic physical GF's. The Kadanoff-Baym equation [20] derived in the real-time formalism [19] is an equation for the equal time GF $G^<(t, t)$. The right-hand side (r.h.s.) of the equation contains in the scattering self-energies the two-time kinetic component of the GF. To close the equations one uses a generalized Kadanoff-Baym ansatz which expresses approximately the off-diagonal kinetic GF in terms of a product of off-diagonal spectral functions and a time-diagonal kinetic GF. In our matrix formalism, the generalized Kadanoff-Baym ansatz is [19]

$$G^<_{ij}(t, t') = i \sum_l \left(G^r_{il}(t, t') G^<_{lj}(t', t') - G^<_{il}(t, t) G^a_{lj}(t, t')_{lj} \right). \quad (10)$$

In the Popov approximation, there are no equal-time kinetic anomalous functions, i.e., no anomalous populations are included: $G^<_{ij}(t, t) = G^<_{ii}(t, t)\delta_{ij}$. These are the main ingredients with which a quantum Boltzmann equation for the bogolons can be derived starting from the Kadanoff-Baym equation for $G^<_{11}(t, t)$. For a detailed description of this approach, see Griffin *et al.* [6].

The spectral functions of a condensed system in the Bogoliubov-Popov approximation are described in Appendix A. In Appendix B, we briefly describe how the Bogoliubov spectrum is modified in terms of dissipative self-energies due to the coupling of a nonresonant pump reservoir. Our GF results agree with corresponding results derived from a Gross-Pitaevskii equation coupled to a reservoir rate equation by Wouters and Carusotto [1] and by Szymanska, Keeling, and Littlewood [9].

As Griffin *et al.* [6] have shown, one has to eliminate the rapidly varying condensate phase $\theta(R, T)$ by a unitary transformation before one can make a power expansion in terms of derivatives with respect to the slowly varying coordinates. The commutator on the left-hand side of the Kadanoff-Baym equation yields after a frequency integration

$$\frac{\partial n_{b,k}}{\partial T} + \frac{\nabla_k}{\hbar}(e_k + \hbar k \cdot v_s)\nabla_R n_{b,k}$$
$$- \nabla_R(e_k + \hbar k \cdot v_s) \cdot \frac{\nabla_k}{\hbar} n_{b,k} = \frac{dn_{b,k}}{dT}\bigg|_{\text{scatt}}, \quad (11)$$

where $n_{b,k} = n_b(k, R, T)$ is the bogolon distribution function and $v_s = \nabla\theta(R, T)\hbar/m_0$ is the condensate velocity. This expression is simply the total time derivative of the distribution function well-known from the Boltzmann classical kinetic theory for dilute gases in a moving frame. The shift term $\hbar k \cdot v_s(R, T)$ can be understood classically as a momentum transform to a moving frame $k' = k - mv_s/\hbar$ from the Boltzmann equation (3) with no external potential $U(R, T)$. The transformation to the moving frame is necessary because the

boson scattering integrals—which we will describe next—will cause a relaxation towards the lowest momentum states $k \to 0$. However, the condensate is moving with the momentum $m_0 v_s$. To eliminate this mismatch, one has to make a transformation t the moving frame.

The various scattering processes have to be described by direct and exchange scattering self-energies as worked out by Griffin *et al.* [6]. Independently Gust and Reichl [7] also derived the scattering rates of the bogolons, based on a density matrix approach developed originally by Kirkpatrick and Dorfman [21]. As far as we can check the results of both groups agree. In the following, we will use the scattering rate in the form of Ref. [7] because they are written in a well-organized and reliable form derived directly using a computer algorithm: These scattering rates for the collision of two bogolons—compare Eq. (4)—have two contributions

$$\frac{dn_{b,k_1}}{dT}\bigg|_{b-b} = \frac{dn_b(k_1)}{dT}\bigg|_{b-b}^{2-2} + \frac{dn_b(k_1)}{dT}\bigg|_{b-b}^{1-3}. \qquad (12)$$

The first term describes the usual number-conserving bogolon-bogolon scattering, while the second term describes the scattering between states with one bogolon and three bogolons.

$$\frac{dn_b(k_1)}{dT}\bigg|_{b-b}^{2-2} = -\frac{4\pi}{\hbar} \sum_{k_2,k_3,k_4}$$

$$\times g^2 \delta_{k_1+k_2,k_3+k_4} \delta(\omega_{k_1}+\omega_{k_2}-\omega_{k_3}-\omega_{k_4})\big(F_{1,2;3,4}^{2-2}\big)^2$$

$$\times (n_b(k_1)n_b(k_2)(1+n_b(k_3))(1+n_b(k_4))$$

$$- (1+n_b(k_1))(1+n_b(k_2))n_b(k_3)n_b(k_4)), \quad (13)$$

where

$$F_{1,2;3,4}^{2-2} = u_1 u_2 u_3 u_4 + u_1 v_2 u_3 v_4 + u_1 v_2 v_3 u_4$$

$$+ v_1 u_2 u_3 v_4 + v_1 u_2 v_3 u_4 + v_1 v_2 v_3 v_4 \qquad (14)$$

is the amplitude of the spectral weight factor. We used the short hand notation $u_i = u(k_i)$, $v_i = v(k_i)$.

The momentum dependence of the interaction matrix element g caused by the polariton Hopfield coefficients has been neglected for simplicity. It should also be noted that the contribution of the phonon scattering to the bogolon relaxation kinetics is not included.

Except for the vertex corrections F^{2-2} the result has the same structure as the semi-classical rate equation. The vertex corrections are given by products of u_k and v_k, which stem from the spectral Beliaev GF's used in the generalized Kadanoff-Baym ansatz for the kinetic GF's in the scattering rates. The four propagators of the two incoming and two outgoing particles enter into the scattering rate of the form $\Sigma^< G^>$. In the ultracold atom literature [6], this scattering rate is called $C_{22}[f]$, because two bogolons are scattered into two other bogolon states. The fact that the absolute square of $F_{1,2,3,4}^{2-2}$ enters into the scattering rate shows that whatever the value of the u's and v's are the effective interaction matrix element squared $g^2(F_{1,2,3,4}^{2-2})^2$ remains always positive as it should. Note that the spectral weight factor reduces without a condensate to 1, because $u_i \to 1$, $v_i \to 0$.

Because the Bogoliubov transformation is not number-conserving and negative energy branches result, there are also terms in which one bogolon is scattered into three and vice versa. Their scattering rate is

$$\frac{dn_b(k_1)}{dT}\bigg|_{b-b}^{1-3} = -\frac{4\pi}{\hbar} \sum_{k_2,k_3,k_4} g^2 \frac{1}{3}$$

$$\times \delta_{k_1,k_2+k_3+k_4} \delta(\omega_{k_1}-\omega_{k_2}-\omega_{k_3}-\omega_{k_4})\big(F_{1,2;3,4}^{1-3}\big)^2$$

$$\times [n_b(k_1)n_b(k_2)n_b(k_3)(1+n_b(k_4))$$

$$- (1+n_b(k_1))(1+n_b(k_2))(1+n_b(k_3))n_b(k_4)], \qquad (15)$$

where

$$F_{1,2;3,4}^{1-3} = u_1 u_2 u_3 v_4 + u_1 u_2 v_3 u_4 + u_1 v_2 u_3 u_4$$

$$+ v_1 v_2 v_3 u_4 + v_1 v_2 u_3 v_4 + v_1 u_2 v_3 v_4. \qquad (16)$$

These scattering rates may be important to change the number of excitations. This term is labeled usually as $C_{13}[f]$, but to our knowledge, their role for the bogolon kinetics has not been investigated in detail. Note that $F^{\{1-3\}} \to 0$, if $n_0 \to 0$. In atomic condensed gases this scattering rate plays a minor role because the gas of excitations is often close to thermal equilibrium. For condensed microcavity polaritons, this scattering process may be more important because these systems are further from equilibrium.

For the scattering between the excitations b and the condensate c, one gets

$$\frac{dn_b(k_1)}{dT}\bigg|_{b-c}^{1-2} = -\frac{4\pi}{\hbar} \sum_{k_2,k_3} g^2 |\Psi(R,T)|^2$$

$$\times \big[2\delta_{k_1+k_2,k_3} \delta\big(\omega_{k_1}+\omega_{b,k_2}-\omega_{k_3}-\omega_c\big)$$

$$\times \big(F_{k_1,k_2,k_3}^{1-2}\big)^2 (n_b(k_1)n_b(k_2)(1+n_b(k_3))$$

$$- (1+n_b(k_1))(1+n_b(k_2))n_b(k_3))$$

$$+ \delta_{k_1,k_2+k_3} \delta\big(\omega_{k_1}+\omega_-\omega_{b,k_2}-\omega_{k_3}\big)$$

$$\times \big(F_{k_3,k_2,k_1}^{1-2}\big)^2 (n_b(k_1)(1+n_b(k_2))(1+n_b(k_3))$$

$$- (1+n_b(k_1))n_b(k_2)n_b(k_3))\big]. \qquad (17)$$

where the vertex correction F_{k_1,k_2,k_3}^{1-2} is given by the symmetrized product of the three involved Bogoliubov coefficients

$$F_{k_1,k_2,k_3}^{1-2} = u_1 u_2 u_3 - u_1 v_2 u_3$$

$$- v_1 u_2 u_3 + u_1 v_2 v_3 + v_1 u_2 v_3 - v_1 v_2 v_3. \qquad (18)$$

This scattering rate is also called Beliaev-Landau scattering. Again the result differs from the semiclassical form only by the vertex correction in terms of symmetrized products of the u, v coefficients. This term is usually called $C_{12}[f]$ because two bogolons are scattered one into the condensate and the other into another state of the excitations. This scattering rate which determines the growth and decay of the condensate has been analyzed best in the literature of atomic gases. However generally speaking—compared to atomic condensates which are mostly close to equilibrium—nonequilibrium properties and quantum-kinetic effects are much more prominent in the nonresonantly pumped micro-cavity polariton systems.

Finally, the scattering from the reservoir into the excited states is deduced from a scattering self-energy diagram with three nondegenerate reservoir lines. The result is

$$
\begin{aligned}
\frac{dn_b(k)}{dT}\bigg|_{r-b} = &-\frac{2\pi}{\hbar}\sum_{k',q} g^2_{r-b,q} \\
&\times \delta(\omega_{b,k} + e_{r,k'} - e_{r,k-q} - e_{r,k'-q})u_k^2 \\
&\times (n_b(k)n_r(k')(1+n_r(k+q))(1+n_r(k'-q)) \\
&- (1+n_b(k))(1+n_r(k'))n_r(k+q)n_r(k'-q)).
\end{aligned}
$$
(19)

Here, only the spectral function u_k^2 enters this scattering rate because only the bogolon GF G_{11} enters into the product of the scattering-self-energy and the GF. Gain is obtained from the second line of the population factors if a reservoir particle with momentum $k+q$ is scattered into a bogolon state with momentum k, while another reservoir particle with momentum $k'-q$ is scattered into an unoccupied state $n_{k'} = 0$, so that the reverse process is not possible. This completes the scattering rates of the bogolon kinetics.

III. NONEQUILIBRIUM GROSS-PITAEVSKII EQ COUPLED TO BOGOLONS

Next, we formulate the equation for the condensate wave function coupled to the excitations above the condensate following the diagrammatic approach of Ref. [4]. Additionally to the self-interaction within the condensate, we take the Hartree-Fock interaction with the bogolons into account as discussed above. The coupling term is given by the difference of the scattering self-energies $\Sigma^>_{\frac{1}{2}} - \Sigma^<_{\frac{1}{2}}$ according to Eq. (8) of Ref. [4]. The resulting nonequilibrium Gross-Pitaevskii equation is

$$
\begin{aligned}
&\left(i\hbar\frac{\partial}{\partial T} + \frac{\hbar^2\nabla^2}{2m_c} - U(R,T) - g_0|\Psi(R,T)|^2\right)\Psi(R,T) \\
&= 2g_0\big(n_b(R,T) + N_r(R,T)\big)\Psi(R,T) \\
&+ \frac{i\hbar}{2}(R_c + iP_c - \gamma_c)\Psi(R,T),
\end{aligned}
$$
(20)

where we have taken the Hartree-Fock exchange energy due to the interaction with the bogolons and the reservoir excitons into account. In a stationary and homogeneous situation, the chemical potential is in accordance with (A18) $\mu = n_0 g_0 + 2g_0 n_b$. The real and imaginary parts of the scattering amplitude R_c and P_c are given by the sum of contributions from the bogolons to the condensate and by the direct scattering from the reservoir into the condensate

$$
R_c = R^{c-b} + R^{c-r}, \quad P_c = P^{c-b} + P^{c-r},
$$
(21)

where

$$
R^{c-b} = -\sum_k \frac{dn_b(k)}{dT}\bigg|_{b-c}^{1-2}\frac{1}{|\Psi(R,T)|^2},
$$
(22)

because of particle conservation and

$$
P^{c-b} = -\sum_k \frac{dn_b(k)}{dT}\bigg|_{b-c}^{1-2}\frac{1}{|\Psi(R,T)|^2}\bigg|_{\pi\delta(\Delta e)\to P(\Delta e)}.
$$
(23)

The imaginary part of the scattering amplitude P^{c-b} describes the dispersive shift connected with the $c-b$ scattering rate [22]. It is obtained by adding a principal value integral to the expressions with the energy conserving delta-functions in (17) using the Dirac identity $1/(\Delta e - i\gamma) \to i\pi\delta(\Delta e) + P(1/\Delta e)$. For a direct scattering from the reservoir into the condensate, the corresponding complex scattering amplitude $R^{c-r} + P^{c-r}$ has been given in Ref. [4]. The GP equation still is a homogeneous equation, which requires a dynamical symmetry breaking, e.g., in terms of fluctuations or at least with a small but finite initial value for the condensate wave function. As for the Boltzmann equation, we will transform the GP equation to the moving coordinate system by writing $\Psi(r,t) = |\Psi(r,t)|\exp(i\Theta(r,t))$, where the amplitude $|\Psi(r,t)|$ is the condensate wave function in the moving frame. Its equation can simply be obtained from (20).

Because we concentrate on the bogolon kinetics, we treat the reservoir by a simple rate equation.

$$
\begin{aligned}
\frac{dN_r(R,T)}{dT} = &P(R,T) - \gamma_r N_r - \sum_k \frac{dn_b(k)}{dT}\bigg|_{r-b} \\
&- \frac{dN_r}{dT}\bigg|_{r-c},
\end{aligned}
$$
(24)

where the reservoir-bogolon scattering rate is given by (19). The reservoir-condensate scattering rate has been given in Ref. [4].

IV. TIME-RESOLVED LUMINESCENCE

As already mentioned the linear Bogoliubov spectrum of the polaritons has been observed in luminescence measurements of Utsunomiya [23]. Recent time-resolved luminescence experiments [10,24] have seen the luminescence from the negative branches (ghost branches), as well. The possibility of observing ghost branch luminescence has been analyzed before by Byrnes et al. [25]. In our context, the momentum, frequency, time- and space-resolved luminescence spectrum can be obtained from the particle correlation function $G^<_{11}(k,\omega,R,T)$. The negative frequency part of $G^<_{11}$ needs for the calculation of the luminescence special consideration. Due to the negative energy eigenvalues with respect to the condensate, the two times on the Keldysh time contour of the nonequilibrium GF are effectively reversed. Thus for the term proportional to v_k^2 one has to replace $G^<_{11} \longrightarrow -G^>_{11} = i(n_{b,k}+1)A_{11}$, so that one gets the following luminescence spectrum:

$$
I(k,\omega,R,T) = |C_k|^2\left(\frac{2\Gamma u_k^2 n_{b,k}}{(\omega - \omega_{b,k})^2 + \Gamma^2} + \frac{2\Gamma v_k^2(n_{b,k}+1)}{(\omega + \omega_{b,k})^2 + \Gamma^2}\right).
$$
(25)

For an equilibrium theory with temperature-dependent GF's of the luminescence of condensed excitons, the negative frequency had to be taken into account in the frequency-dependent Bose distribution: $n(-\omega) = 1/(e^{-\beta\omega} - 1) = -(n(\omega) + 1)$, as used by one of us [26,27]. This replacement yielded again a spectrum of the form (25).

With the discussed reformulation for the negative frequency part, the luminescence spectrum is positive definite,

as it should be. The result (25) agrees with the result of Byrnes *et al.* [25]. The first term yields the normal luminescence which can also be observed below the condensation threshold, while the second term describes the ghost branch luminescence which is only present in the condensed phase. C_k is again the Hopfield coefficient for the photon component of the polariton because only the photon component can emerge from the cavity. The luminescence spectrum can also be seen as bogolon-assisted photon emission processes of the condensate. The first term describes the radiative decay of a condensed particle simultaneously absorbing a bogolon ($\propto n_{b,k}$), and the second term is due to the emission of a photon and the spontaneous and stimulated emission of a bogolon ($\propto (1 + n_{b,k})$).

Thus with the results of our quantum kinetics, we can at the same time determine temporal development of the polariton luminescence. The measured luminescence spectrum close to the condensate has been inspected by Assmann *et al.* [28] but a conclusive result about the modification has not been obtained. The recently observed ghost branch luminescence high above the condensate threshold [23] is not based on specific nonequilibrium modifications of the Bogoliubov spectrum but is rather natural for a Bose condensed system.

The Bogoliubov coefficient v_k describes the coupling of the condensate to a pair of bogolons with opposite momenta. This process is for higher momentum states responsible for the depletion of the condensate. The resulting scaling of the ghost branch spectrum which is due to depletion of the condensate has recently been observed by Pieczarka *et al.* [16].

Future luminescence measurements of the excited states with improved resolution may allow detecting the nonequilibrium modifications of the bogolon spectrum for small k values.

V. NUMERICAL RESULTS

In this section, we present numerical solutions of the following set of coupled equations: (a) the reservoir rate equation (24), (b) the bogolon quantum Boltzmann equation (3), and (c) the Gross-Pitaevskii equation for the condensate wave function (20). The nonresonant Gaussian pump beam which excites the reservoir

$$P(R, T) = P_0 e^{-(R/R_0)^2} \tanh(T/T_0) \quad (26)$$

is switched on in $T_0 = 1$ ps and has a radius of $R_0 = 3$ μm. The stationary pump power for all shown results is $P_0 = 1.5 P_c$, where P_c is the threshold pump power. We will use the parameters of a CdTe-type microcavity with a quadratic cross-section of length $L = 12.6$ μm. The spectrum of the excitation is limited to $k_1 \leqslant k \leqslant 2$ μm^{-1} because at the higher border the dispersions of the bogolons and the reservoir cut each other. The material parameters used in our calculations are those listed in Ref. [22]. The numerical evaluations have been performed using 64×64 grid points in real space and 9×9 grid points in momentum space.

For the solution of the Gross-Pitaevskii equation (33), we use the split-step Fourier transform by writing the condensate wave function as

$$\Psi(R, T + dT) = i\mathcal{F}^{-1}\left\{ e^{-i\frac{\hbar k^2}{2m}dT} \mathcal{F}\left[e^{-i\frac{V(R,T)}{\hbar}dT} \Psi(R, T) \right] \right\}, \quad (27)$$

where $V(R, T)$ is given by

$$V(R, T) = g\left[|\Psi(R, T)|^2 + 2\left(\sum_k n_b(k, R, T) + N_r(R, T) \right) \right]$$
$$+ \frac{i\hbar}{2}(R_c(R, T) + iP_c(R, T) - \gamma_c). \quad (28)$$

Here, $\mathcal{F}$ is the Fourier transform. At $T = 0$, the wave function is initiated with noise

$$\Psi(R, T = 0) = a^{ibr}, \quad (29)$$

where a and b are random variables.

The numerical treatment of the kinetics together with transport is known to be notoriously difficult and leads often to the violation of the particle number conservation [29]. It is therefore essential to reformulate the drift term in such a way that it displays the number conservation explicitly.

$$\left. \frac{\partial n_b(R, k)}{\partial T} \right|_{\text{drift}} = (\nabla_k/\hbar)(e_k + \hbar k \cdot v_s) \cdot \nabla_R n_b(R, k))$$
$$- \nabla_R(e_k + \hbar k \cdot v_s) \cdot (\nabla_k/\hbar) n_b(R, k))$$
$$= \nabla_R \cdot [((\nabla_k/\hbar)(e_k + \hbar k \cdot v_s)) n_b(R, k)]$$
$$- (\nabla_k/\hbar) \cdot [(\nabla_R(e_k + \hbar k \cdot v_s)) n_b(R, k)]$$
$$= \nabla_R j_R(R, k) - (\nabla_k/\hbar) j_k(R, k), \quad (30)$$

with the currents in real and momentum space

$$j_{\binom{R}{k}}(R, k) = \left(\binom{(\nabla_k/\hbar)}{\nabla_R} \right)(e_k + \hbar k \cdot v_s)\right) n_b(R, k). \quad (31)$$

Now we have derived the drift term in the form of a continuity equation. If one takes the 2D volume integrals over the r and k space, one gets for the first term with the Gauss law a surface integral over the sample with the normal components of the current $j_{1,n}$. These currents are zero on the surface. Similarly the second term yields after the k integration a surface integral in k space, again these integrals vanish so that the total bogolon number is conserved by the drift term:

$$\left. \frac{\partial N_b(T)}{\partial T} \right|_{\text{drift}} = 0. \quad (32)$$

With this formulation, one can follow the procedure of Smolarkiewicz [29], where a small diffusion term is added to guarantee stability for the numerical evaluation on a discrete lattice.

Figure 2 shows the resulting build-up of the condensate population $N_0(T) = \int d^2R n_0(R, T)$ (red line), and the excited states, i.e., the total number of bogolons $N_b(T) = \int d^2R \sum_k n_{b,k}(R, T)/S$ (green line). The area S is that of the inner square where the condensate is mostly concentrated, as will be discussed in more detail when we present the spatial distribution of the condensate and the excitations below. Here $n_0(R, T)$ is the condensate density, while $n_{b,k}(R, T)$ is the number of excitations at a given momentum, position, and time. For the chosen pump strength of $1.5 P_c$ above the critical pump strength P_c, one sees first a rapid build-up of the excitations at about 0.1 ns. Because the switch-on time of 1 ps is much shorter than the exciton or photon cavity lifetime, a pronounced over-shoot of the number of excitations $N_b(T)$ occurs, followed by a stationary region which is determined
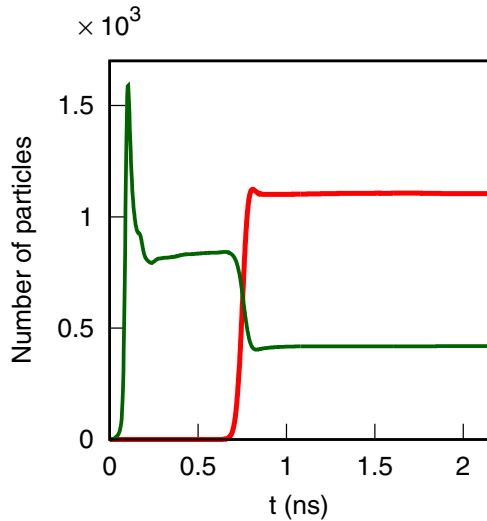
FIG. 2. Time development of the number of particles in the condensate $N_0(T) = \int d^2R\, n_0(R, T)$ (red line) and number of all bogolons $N_b(T) = \int d^2R \sum_k n_{b,k}(R, T)/S$ (green line) for a pump power of $P_0 = 1.5P_c$. S has been taken as the area of an inner square where most of the condensate is located.

by the balance of the pump and loss rate. During this time interval, the bogolons still relax toward lower energies until the condensation occurs after about 0.7 ns. After condensation the number of bogolons decrease to their stationary value. In the following, we will show various results of the kinetics for the stationary regime after the condensation.

In Fig. 3, the dispersions (without shifts) are shown for the unperturbed polaritons and the bogolons for the spatial position with the maximal condensate density of 10^{10} cm^{-2}. The inset shows the linear regime of the Bogoliubov-Popov spectrum above condensation. First, we will discuss the spatial distributions of the condensate and the bogolons.

In Fig. 4, the resulting stationary condensate wave function is displayed 2.1 ns after switch-on: the amplitude is described

FIG. 4. Amplitude (contour plot), phase (grey scale) and super-fluid velocity (vector field) of the condensate wave function 2.1ns after onset of the excitation.

in terms of a contour plot with a central dip and 4 peaks in the corners of an inner square, where the condensate is mostly concentrated. In the outer area, one sees a series of smaller maxima parallel to the sides of the sample. The superfluid velocity is shown by arrows, with a fast flow away from the center area to the outer regions. The phase is indicated by a grey scale, with lines of a phase jump where the white and dark areas meet. The ends of these phase jump lines are connected with vortices and antivortices, as will be seen more clearly in the following figure.

In Fig. 5, the flow patterns of the condensate are seen particularly well. The inner region is dominated by a flow away from the center turning in the outer region to areas with
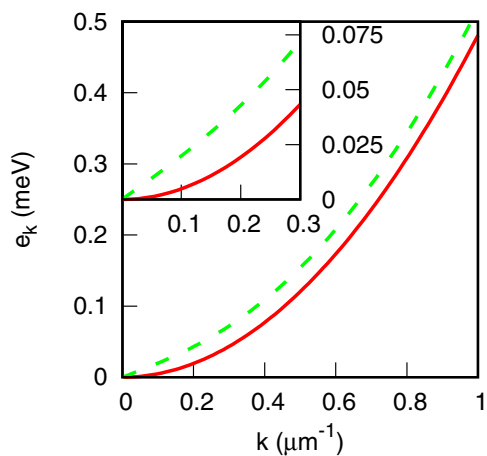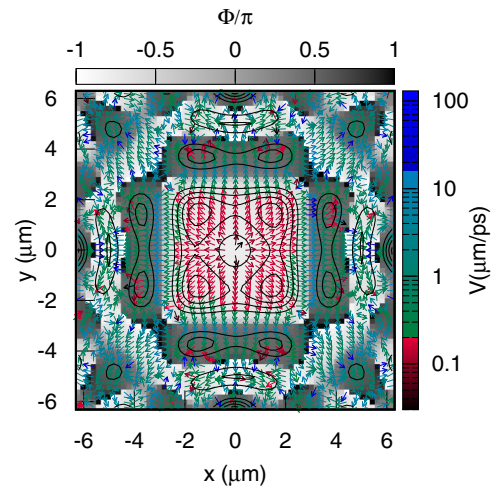

FIG. 3. Dispersion of the unperturbed polaritons (full red line), and that of the bogolons (green dashed line) under stationary conditions for the maximum condensate density of $n_0(R) = 10^{10}$ cm^{-2}. Shifts are not shown. (Inset) Dispersions for small momenta.
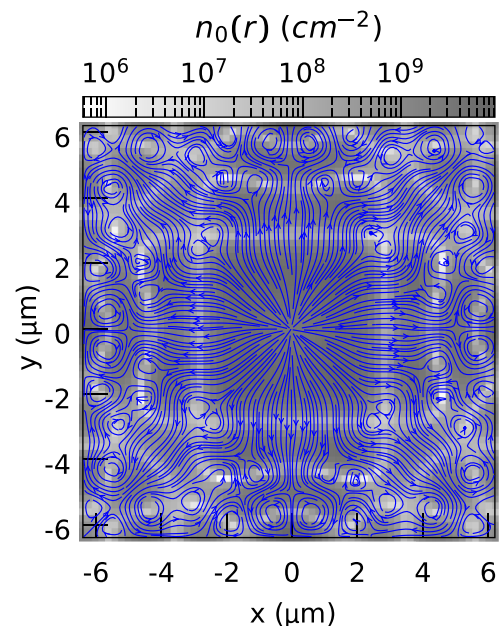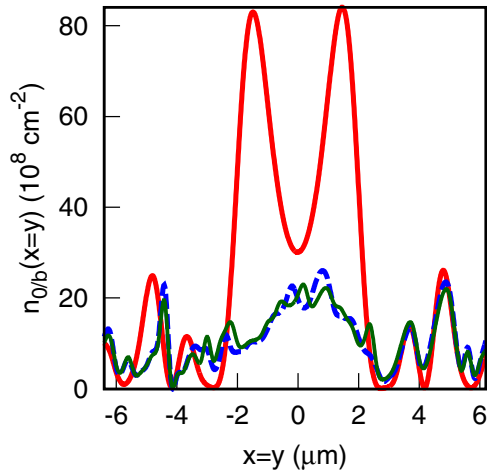

FIG. 5. Streamlines for the condensate flow.

FIG. 6. Condensate distribution $n_0(R)$ (red) along the diagonal of the sample $x = y$ and the corresponding bogolon distribution $n_b(R, T) = \sum_k n_{b,k}(R, T)/S$ 5 ps (green line) and 200 ps (dashed blue line) after condensation.

FIG. 7. Distribution of the bogolon density $n_b(R) = \sum_k n_{b,k}(R)/S$.

pronounced vorticity. Along the boundaries of the sample, a row of vortex-antivortex pairs can be seen.

In Fig. 6, we plot the condensate and bogolon densities along the diagonal $x = y$ of the sample. Here the coherent wave character of the condensate becomes even more evident. The condensate (red line) has a minimum at the center due to the rapid flow of the condensate but also of the bogolons out of this area. The first maximum is reached in the corners of the inner square at about $x = y = \pm 2$ μm, while it has a richer, finer structures in the outer regions, as seen, e.g., from the four relatively pronounced side peaks in the corners of the sample (see also Fig. 4). Because the condensate is mostly confined to the inner square $S = 4.8\,\mu\text{m} \times 4.8\,\mu\text{m}$, we normalized the condensate density with this area. Note that we simplified the problem for the condensate and the excitations by using periodic boundary conditions. This was necessary for the application of the split-step Fourier transform method for the solution of the GPE and using the standard Bogoliubov theory for the excitations. As a consequence, the condensate wave function Ψ at the boundary does not vanish. We also show the bogolon density summed over all k states at two times, showing that their spatial distribution still changes 5 ps after the condensation, while they are already close to a local equilibrium distribution. Note also there is a pronounced deviation from a symmetric bogolon distribution, particularly at early times.

Figure 7 the spatial distribution of all excitations above the condensate $n_b(R, T) = \sum_k n_{b,k}(R, T)/S$ is shown. This distribution has pronounced square patterns, which result from the motion due to the drift terms. The distribution in the central part in between the condensate peaks is relatively smooth and weakly populated by the bogolons, which pile up about 3 μm away from the center. In the regions with pronounced vorticity rapid spatial variations of the bogolon distribution are seen.

An important question is to which degree the bogolons reach a local thermal equilibrium well in the stationary regime. Because in our kinetics phonon scattering is not included, the bogolon temperature is only determined by the
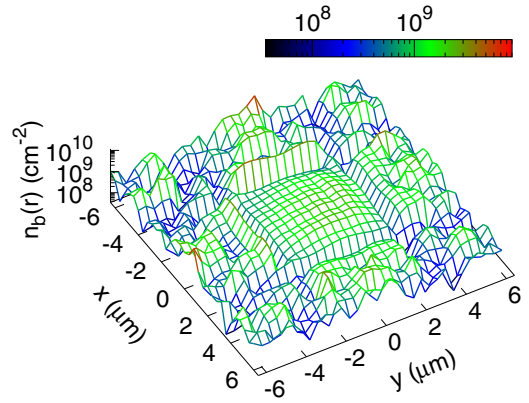
mean energy of the bogolon gas. Experimentally, a thermal equilibrium bogolon distribution has been observed only in microcavities with a trap and with particular long polariton lifetimes ($\simeq$270 ps), even if the excitation occurred outside the trap in which the condensate took place [30].

Because the collision integrals conserve energy, momentum and particle number (at least approximately because the number-conserving scattering rates $dn_b(k)/dT|_{b-b}^{2-2}$ are found to be considerably larger than the number-nonconserving scattering rates $dn_b(k)/dT|_{b-b}^{1-3}$), the local equilibrium Bose-Einstein distribution has in general 3 parameter fields, namely, the inverse temperature $\beta(R, T) = 1/k_B T_b(R, T)$, the drift velocity $v_d(R, T)$, and the chemical potential $\mu(R, T)$.

$$n_k^{le}(R, T) = \frac{1}{e^{\beta(R,T)[e_{b,k}(R,T)-\hbar k \cdot u_d(R,T)-\mu(R,T)]} - 1}. \quad (33)$$

We have already seen from Fig. 7 that there are a relatively homogeneous inner square and a rather structured outer region with considerable vorticity. If local equilibrium would be established everywhere in the sample, one could derive from the quantum Boltzmann equation the equations for the corresponding conserved quantities, i.e., number density, momentum density, and energy density together with the equation for the superfluid velocity v_s. Furthermore one could use the thermodynamic relations between thermodynamic functions that enter these equations. By these means, one could formulate a two-fluid model for the polaritons in analogy to the Landau description of superfluid ^{4}He. So far, however, the observed processes have been too fast for describing them in terms of a two-fluid model.

To check whether the calculated distributions reached at all in the stationary regime, here at 2.1ns after switch-on, we first consider examples of the relatively spatially homogeneous center part, starting with the distribution at the center of excitation, where according to Fig. 6 the condensate has a dip due to the rapid outflow. Thus the left panel of Fig. 8 the calculated bogolon distributions are shown in momentum space for the spatial center point $x = y = 0$. The calculated distributions are marked by symbols, the fits to local equilibrium (33) are shown by lines. To guide the eye, symbols and lines in the k_x direction are plotted in the same color, while in the k_y direction the same symbols are used. It is seen that at this central point the local equilibrium is reached perfectly.
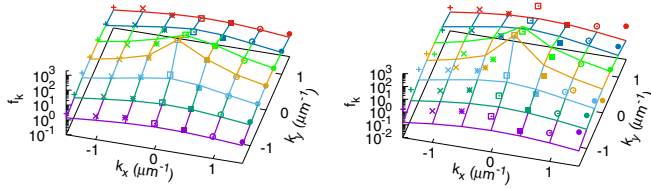
FIG. 8. Fits of the calculated bogolon distribution in k space (symbols) with a local equilibrium distribution (lines). Points with the same k_x value have the same symbols, points with the same k_y value have the same color. The left figure is for the central position $x = 0$, $y = 0$. The right figure is for the example of a small side peak of the condensate at $x = -3.8 \, \mu$m, $y = -1.4 \, \mu$m.

A second example is given in the right part of Fig. 8 for a small side peak of the condensate at the position $x = -3.8 \, \mu$m, $y = -1.4 \, \mu$m. Also at this position, the fit of the local equilibrium distribution to the calculated distribution works reasonably well.

In the outer regions of the sample, the bogolon distributions exhibit relatively large spatial variations and considerable vorticity. In Fig. 9, fits of the calculated bogolon distribution to the local equilibrium distribution are shown for positions in which a relatively large drift velocity shifts the peak of the local equilibrium distributions appreciably. We show in the left part of Fig. 9 an example for the position $x = -4.6 \, \mu$m, $y = -5.2 \, \mu$m where we obtain a drift velocity in x direction corresponding to a drift momentum $k_{d,x} = 0.2 \, \mu$m^{-1}. In the right part of Fig. 9, we show for the position $x = -2.2 \, \mu$m, $y = -3 \, \mu$m an example which yields the large drift vector $k_{d,x} = 0.96 \, \mu$m^{-1}. Still, the fits to local equilibrium are possible but they get less accurate for larger drift velocities.

Next, we present at least for the inner area where the fits to the local equilibrium distributions are quite good the resulting parameter fields. In Fig. 10, we show the resulting drift velocity field $u_d(R)$ and compare this velocity field of the excitations with the superfluid velocity field of the condensate $v_s(R)$ given by thick arrows. In general, the two velocity fields are closely related, but one finds also regions with strong differences. In Fig. 11, the resulting chemical potential $\mu(R)$ is shown. In the region surrounding the inner condensate minimum (with a slight asymmetry to the left) the chemical potential takes larger negative values which indicate
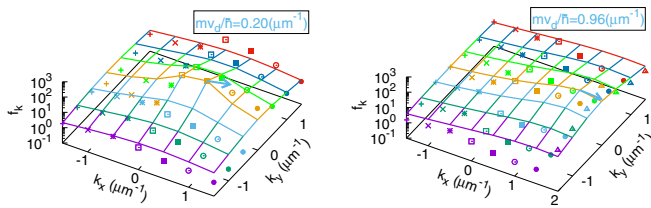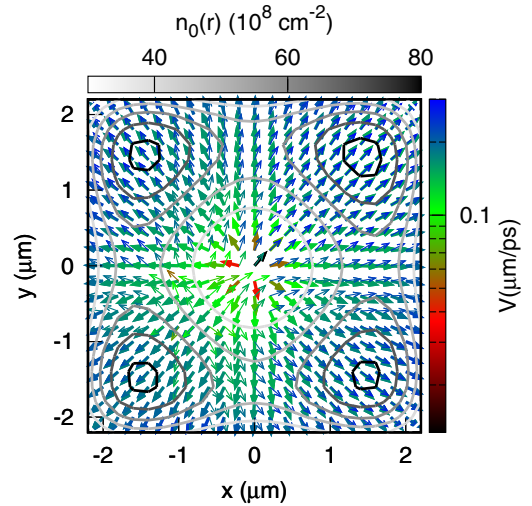

FIG. 10. Local drift velocities of the bogolons (thin vector field lines). For comparison also the superfluid velocity field v_s is shown by the thick vector field lines.

a classical region rather than a quantum phase region, while it approaches zero in the vicinity of the condensate peaks. In Fig. 12, the resulting temperature is plotted. Consistent with the results for the chemical potential we find the highest temperatures in the regions where the bogolon gas is most classical, and low temperatures in the vicinity of the condensate peaks. Finally, we show in Fig. 13 the fitting parameters along the diagonal $x = y$. Here we see again that μ, T, and u_d are strongly varying functions of the position. In the center where the condensate has a minimum the chemical potential has large negative values and the local temperature is correspondingly high. Around the maxima of the condensate population, μ approaches zero and the temperature is low. The drift velocity (green arrows) follow more or less the superfluid velocity (red arrows).

With these results, we have shown that under stationary conditions at least in the regions without large spatial variations of the condensate wave function and the bogolon distributions the excitations above the condensate reach a

FIG. 9. Fits of the calculated bogolon distribution in k-space (symbols) with a local equilibrium distribution (lines) at the edge of the vorticity zone. The left figure is calculated for $x = -4.6 \, \mu$m, $y = -5.2 \, \mu$m. The fits yield a drift velocity corresponding to a momentum of $k_d = 0.2 \, \mu$m^{-1}. The left figure is calculated for the position $x = -2.2 \, \mu$m, $y = -3 \, \mu$m. A drift velocity corresponding to the momentum of $k_d = 0.96 \, \mu$m^{-1} is obtained.
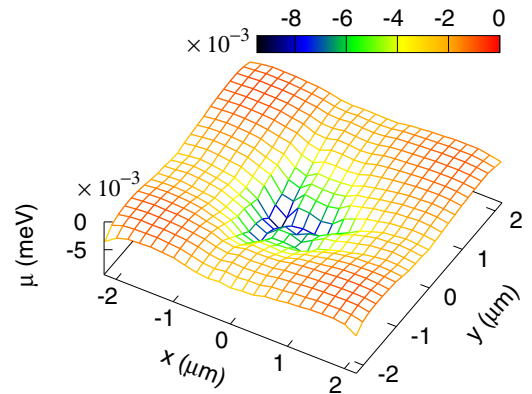

FIG. 11. Chemical potential of the bogolon gas obtained from fits to a local equilibrium distribution.
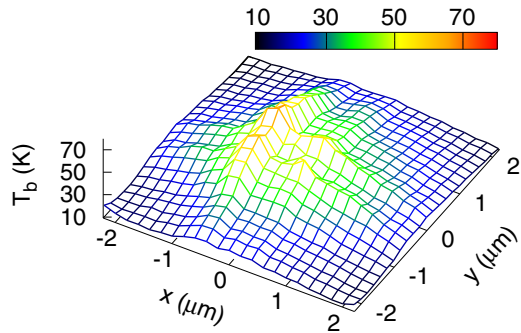
FIG. 12. Temperature of the bogolon gas obtained from fits to a local equilibrium distribution.

FIG. 14. Normalized bogolon luminescence plotted in a logarithmic scale before the onset of condensation (left part) and after the onset of condensation (right part), respectively.

local equilibrium, while in the strongly structured regions a fit to local equilibrium distributions was getting less accurate.

Finally, we want to present the resulting luminescence spectra in Fig. 14. Below the onset of condensation (see the left part of Fig. 14) only the upper branch of the luminescence spectrum is seen with a mainly quadratic spectrum. Above condensation (see right part of Fig. 14) both the positive branch on the high-frequency side of the condensate as well as the negative branch, also called the ghost branch, are visible and resemble the spectra which have been observed [15,16]. In practice, the observation of the relatively weak bogolon luminescence is difficult because of the proximity to the strong condensate luminescence. As discussed above the bogolon luminescence can alternatively be understood as an optical decay of a condensate particle assisted by the absorption of a bogolon on the high-energy side, and assisted by the spontaneous and stimulated emission of a bogolon below the condensate line. Because the ghost branch is proportional to the square of the Bogoliubov coefficient v_k which is proportional to the condensate density it is, in particular, a strong signature of the presence of a polariton BEC.

In conclusion, we have extended the treatment of BE condensed exciton polaritons in semiconductor microcavities by including the k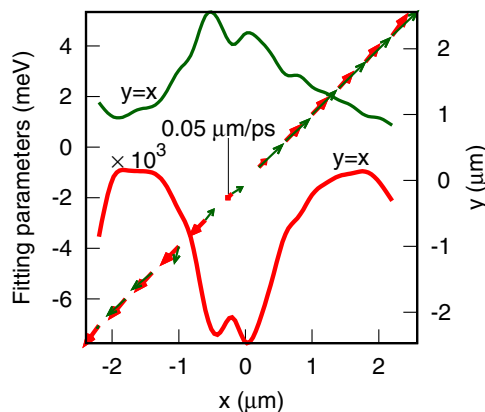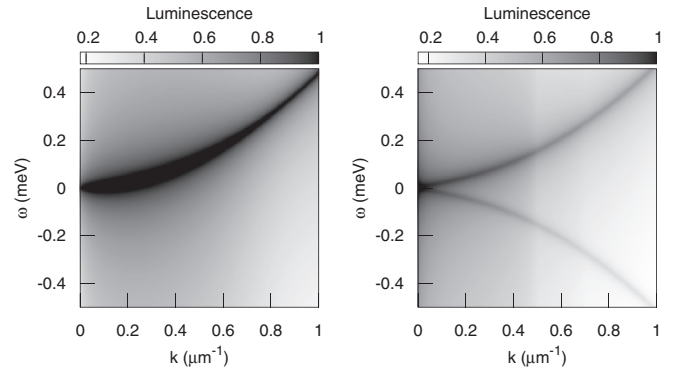inetics of the excitations above the condensate, called bogolons. We have shown the bogolons reach under stationary excitations local equilibrium only partially, namely, only in regions with weak spatial variations. The results of the bogolon kinetics yield directly the time- and space-resolved luminescence spectrum including the ghost branch. We did not intend to adjust details of the bogolon-condensate kinetics to get an agreement with available experimental observations, e.g., by introducing also the scattering by phonons, but tried to demonstrate the basic features of the coupled bogolon-condensate kinetics.

APPENDIX A: SPECTRAL GREEN FUNCTIONS IN THE BOGOLIUBOV-POPOV APPROXIMATION

We briefly discuss the retarded GF's for a condensed boson system in equilibrium and a general nonequilibrium system. After a Fourier transform with the spatially rapidly varying relative coordinates are with $\psi(r, t) = \sum_k a_k(t)e^{ik \cdot r}$ suppressing for simplicity the vector notation the normal and anomalous retarded GF's are defined as

$$G_{11,k}^r(t, t') = -i\Theta(t - t')\langle[a_{1,k}(t), a_{1,k}^\dagger(t')]\rangle$$
$$= -i\Theta(t - t')\langle[a_k(t), a_k^\dagger(t')]\rangle \quad (A1)$$

and

$$G_{12,k}^r(t, t') = -i\Theta(t - t')\langle[a_{1,k}(t), a_{2,k}^\dagger(t')]\rangle$$
$$= -i\Theta(t - t')\langle[a_k(t), a_{-k}(t')]\rangle . \quad (A2)$$

This function is called pair function or anomalous GF. For a mean-field self-energy

$$\Sigma_k(t, t') = \Sigma_k(t)\delta(t - t'), \quad (A3)$$

FIG. 13. Chemical potential μ (red line), temperature k_BT (green line) and drift velocity (green arrows) and superfluid velocity (red arrows) along the diagonal $x = y$.

the retarded GF's obey the following equations:

$$i\frac{\partial G^r_{11,k}(t,t')}{\partial t}\bigg|_{mf} = \delta(t-t') + (e_k + \Sigma_{11,k}(t))G^r_{11,k}(t,t')$$

$$+ \Sigma_{12,k}(t)G^r_{21,k}(t,t'),\qquad (A4)$$

where $G^r_{21,k}(t,t') = G^{r*}_{12,k}(t,t')$. For the retarded off-diagonal GF $G^r_{12,k}(t,t')^*$ we get

$$i\frac{\partial G^r_{12,k}(t,t')}{\partial t}\bigg|_{mf} = (e_k + \Sigma_{11,k}(t))G^r_{12,k}(t,t')$$

$$+ \Sigma_{12,k}(t)G^r_{22,k}(t,t').\qquad (A5)$$

The singular mean field-self-energies in the Hartree-Fock-Popov approximation are

$$\Sigma_{11}(t) = 2g_0(n_0(t) + n_b(t)) \text{ with } n_b(t) = \sum_{k\neq 0} n_b(k,t),$$
$$(A6)$$

$$\Sigma_{12} = g_0 \Psi_0^2(t).\qquad (A7)$$

In stationary equilibrium, the order parameter oscillates with the chemical potential μ like

$$\Psi_0(t) = e^{-i\mu t}\Psi_0(t)^{st} = e^{-i\mu t}\sqrt{n_0}.\qquad (A8)$$

The anomalous self-energy varies thus under stationary conditions

$$\Sigma_{12}(t) = e^{-i2\mu t}\Sigma_{12}^{st}.\qquad (A9)$$

To reach a stationary solution for the two nonequilibrium Dyson equations the stationary solutions of the spectral functions have to vary as

$$G^r_{12,k}(t,t') = e^{i\mu(t+t')}G^{r,st}_{12,k}(t,t'),$$
$$G^r_{11,k}(t,t') = e^{-i\mu(t-t')}G^{r,st}_{11,k}(t,t'),\qquad (A10)$$

i.e., all energy has to be shifted by the chemical potential. This corresponds to a transition to a grand canonical Hamiltonian which guarantees the conservation of the mean particle number in equilibrium. Using the symmetry properties of the GF's, the corresponding Dyson equations for a stationary equilibrium system take the standard textbook form

$$i\frac{\partial G^{r,st}_{11,k}(t,t')}{\partial t}\bigg|_{mf} = \delta(t-t') + (e_k - \mu + \Sigma^{st}_{11,k}(t))G^{r,st}_{11,k}(t,t')$$

$$+ \Sigma^{st}_{12,k}(t)G^{r,st*}_{12,k}(t,t')\qquad (A11)$$

and

$$-i\frac{\partial G^{r,st*}_{12,k}(t,t')}{\partial t}\bigg|_{mf} = (e_k - \mu + \Sigma^{st}_{22,k}(t))G^{r,st*}_{12,k}(t,t')$$

$$+ \Sigma^{st}_{12,k}(t)G^{r,st}_{11,k}(t,t'),\qquad (A12)$$

where we used $G^{r,st*}_{22,k}(t,t') = G^{r,st}_{11,k}(t,t')$. Naturally the upper index st—which we introduced for clarity—is in the conventional equilibrium theory not written explicitly. After a Fourier transformation, these functions can be put into the form

$$G^r_{11}(k,\omega) = \frac{u_k^2}{\omega - \omega_{1,k} + i\gamma} - \frac{v_k^2}{\omega - \omega_{2,k} + i\gamma}\qquad (A13)$$

and

$$G^r_{12}(k,\omega) = -\frac{u_k v_k}{\omega - \omega_{1,k} + i\gamma} + \frac{u_k v_k}{\omega - \omega_{2,k} + i\gamma}\qquad (A14)$$

with the Bogoliubov coefficients with $u_k^2 - v_k^2 = 1$

$$u_k^2 = \frac{1}{2}\left(\frac{e_k + g_0 n_0}{\omega_{1,k}} + 1\right),\quad v_k^2 = \frac{1}{2}\left(\frac{e_k + g_0 n_0}{\omega_{1,k}} - 1\right),$$
$$(A15)$$

where the bogolon energies are

$$\omega_{1,2,k} = \pm\sqrt{\left(e_k - \mu + \Sigma^{st}_{11,k}\right)^2 - \left|\Sigma^{st}_{12,k}\right|^2}.\qquad (A16)$$

With the Hugenholtz-Pines theorem [31] $\mu = \Sigma^{st}_{11} - \Sigma^{st}_{12}$ the spectrum for small momenta becomes phononlike

$$\omega_{1,2,k} = \pm\sqrt{e_k^2 + 2e_k \Sigma^{st}_{12}}.\qquad (A17)$$

For the Popov approximation, the Hugenholtz-Pines theorem is automatically fulfilled

$$\mu = \Sigma^{st}_{11} - \Sigma^{st}_{12} = n_0 g_0 + 2g_0 n_b.\qquad (A18)$$

For illustration, in thermal equilibrium, this relation is written with the total number of particles $n = n_0(T) + n_b$ yields

$$\mu = 2n g_0 - n_0(T)g_0 = n g_0\left(1 + \left(\frac{T}{T_c}\right)^{\frac{3}{2}}\right),\qquad (A19)$$

where the Popov relation

$$n_0(T) = n - n_b = n\left(1 - \left(\frac{T}{T_c}\right)^{\frac{3}{2}}\right)\qquad (A20)$$

has been used.

Thus one finds a gap-less spectrum

$$\omega_{1,2,k} = \pm\sqrt{e_k^2 + 2g_0 n_0 e_k} = \pm e_{b,k}.\qquad (A21)$$

In contrast to the Bogoliubov approximation, the Popov approximation can be used also in the vicinity of T_c. The only difference is that n_0 is in the Popov approximation replaced in thermal equilibrium by the temperature-dependent $n_0(T)$, or in the kinetic theory by the self-consistently calculated condensate population n_0 which is in general still a slowly varying function of the central space and time coordinates. We will use the spectral functions in the Popov approximation for the development of the kinetics. With weak spatial and temporal variations of the condensate density the spectral functions also become functions of R and T: $G^r(R,T,k,\omega)$ and $G^a(R,T,k,\omega)$, respectively. Because the boson condition is $u_k^2 - v_k^2 = 1$, one can express these coefficients in terms of hyperbolic functions:

$$u_k = \cosh(\varphi_k),\quad v_k = \sinh(\varphi_k).\qquad (A22)$$

APPENDIX B: NONEQUILIBRIUM MODIFICATION OF THE SPECTRAL FUNCTIONS

Finally, we want to treat the modifications of the eigenmodes by the coupling to the reservoir which has been derived from the Gross-Pitaevskii equation [1,9]. For this purpose, we consider two limits of the ratio of the lifetimes of the excitons in the reservoir and the polaritons in the ground state.

1. Short reservoir lifetime

If the lifetimes of the reservoir excitons are short in comparison to the cavity lifetime one can at least approximately eliminate the reservoir variable adiabatically. This case has been considered in the previous investigations of Symanska *et al.* [9] and Wouters, Carusotto [1] in terms of a nonequilibrium Gross-Pitaevskii equation. Here we consider the dissipative parts of the self-energies of the retarded GF's due to the coupling to the reservoir:

$$\Sigma_{11}'' = \Sigma_{12}'' = -i\Gamma . \tag{B1}$$

From (A11) and (A12), one gets

$$(\omega - (e_k + n_0 g_0 - i\Gamma)G_{11}^r + (n_0 g_0 - i\Gamma)G_{12}^{r*} = 1,$$

$$(n_0 g_0 + i\Gamma)G_{11}^r + (\omega + (e_k + n_0 g_0 + i\Gamma)G_{12}^{r*} = 0 . \tag{B2}$$

From the determinant of this system of equations

$$Det = (\omega + i\Gamma)^2 - (e_k + n_0 g_0)^2 + n_0^2 g_0^2 + \Gamma^2 , \tag{B3}$$

one finds the damped eigenfrequencies

$$\omega_{1,2,k}^{ne} = -i\Gamma \pm \sqrt{\omega_{b,k}^2 - \Gamma^2} . \tag{B4}$$

This nonequilibrium spectrum has no real solution for k values smaller than $\omega_{b,k} < \Gamma$. It connects at this point the positive and negative branch of the excitations [1,9]. This modification of the polariton spectrum will be important in connection with the luminescence from the negative branch, also called the ghost branch. The coefficients u_k^2 and v_k^2 given by (A15) remain unchanged, only the modified eigenfrequencies (B4)

have to be inserted instead of the unperturbed Bogoliubov spectrum.

2. Short microcavity lifetime

Typical cavity lifetimes are of the order of 10^{-11} s, i.e., short to typical exciton lifetimes of 10^{-9} s. In this case which has also be considered by Byrnes *et al.* [25], one has the following normal dissipative self-energies:

$$\Sigma_{11}'' = -i\Gamma, \quad \Sigma_{12}'' = 0 . \tag{B5}$$

In this case, we have only diagonal damping terms in (B2), i.e., the infinitesimal damping γ of the retarded GF's is now the finite damping Γ. The resulting nonequilibrium bogolon spectrum is

$$\omega_{1,2,k}^{ne} = \pm\sqrt{\omega_{b,k}^2 + \Gamma^2} . \tag{B6}$$

Now the spectrum has a gap at small k values, the upper branches for negative and positive k values connect smoothly at $k = 0$, and correspondingly for the negative branches.

So far the investigations of the luminescence spectra [28] are not conclusive which of the two nonequilibrium spectra is realized in the best present-day GaAs- or CdTe-type micro-cavities. Thus, in our kinetics, we will use the simple unmodified spectrum (A21), because the main features of the luminescence, including the appearance of the ghost branch, will be shown to be independent of these finer modifications.

---

[1] M. Wouters and I. Carusotto, Excitations in a Nonequilibrium Bose-Einstein Condensate of Exciton Polaritons, Phys. Rev. Lett. **99**, 140402 (2007).

[2] E. P. Gross, Structure of a quantized vortex in boson systems, Il Nuovo Cimento (1955-1965) **20**, 454 (1961).

[3] N. Proukakis, S. Gardiner, M. Davis, and M. Szymańska, *Quantum Gases, Finite Temperature and Non-Equilibrium Dynamics* (Imperial College Press, 2013), p. 70.

[4] H. Haug, T. D. Doan, and D. B. Tran Thoai, Quantum kinetic derivation of the nonequilibrium Gross-Pitaevskii equation for nonresonant excitation of microcavity polaritons, Phys. Rev. B **89**, 155302 (2014).

[5] N. P. Proukakis and B. Jackson, Finite-temperature models of Bose–Einstein condensation, J. Phys. B: At. Mol. Opt. Phys. **41**, 203002 (2008).

[6] A. Griffin, T. Nikuni, and E. Zaremba, *Bose-Condensed Gases at Finite Temperatures*, 1st ed. (Cambridge University Press, Cambridge, New York, 2009).

[7] E. D. Gust and L. E. Reichl, The viscosity of dilute Bose–Einstein condensates, Phys. Scr. **T165**, 014034 (2015).

[8] V. N. Popov, *Functional Integrals in Quantum Field Theory and Statistical Physics*, Mathematical Physics and Applied Mathematics, Vol. 8 (D. Reidel Publishing Company, Dordrecht, Boston, Lancaster, 1983), p. 134.

[9] M. H. Szymanska, J. Keeling, and P. B. Littlewood, Non-Equilibrium Quantum Condensation in an Incoherently Pumped Dissipative System, Phys. Rev. Lett. **96**, 230602 (2006).

[10] G. Roumpos, M. D. Fraser, A. Loeffler, S. Höfling, A. Forchel, and Y. Yamamoto, Single vortex-antivortex pair in an exciton-polariton condensate, Nat. Phys. **7**, 129 (2011).

[11] T. D. Doan, H. T. Cao, D. B. Tran Thoai, and H. Haug, Condensation kinetics of microcavity polaritons with scattering by phonons and polaritons, Phys. Rev. B **72**, 085301 (2005).

[12] H. T. Cao, T. D. Doan, D. B. Tran Thoai, and H. Haug, Polarization kinetics of semiconductor microcavities investigated with a Boltzman approach, Phys. Rev. B **77**, 075320 (2008).

[13] I. A. Shelykh, A. V. Kavokin, and G. Malpuech, Spin dynamics of exciton polaritons in microcavities, Phys. Status Solidi B **242**, 2271 (2005).

[14] F. Manni, K. G. Lagoudakis, T. C. H. Liew, R. André, and B. Deveaud-Plédran, Spontaneous Pattern Formation in a Polariton Condensate, Phys. Rev. Lett. **107**, 106401 (2011).

[15] M. Pieczarka, M. Syperek, Ł. Dusanowski, J. Misiewicz, F. Langer, A. Forchel, M. Kamp, C. Schneider, S. Höfling, A. Kavokin, and G. Sęk, Ghost Branch Photoluminescence from a Polariton Fluid Under Nonresonant Excitation, Phys. Rev. Lett. **115**, 186401 (2015).

[16] M. Pieczarka, E. Estrecho, M. Boozarjmehr, O. Bleu, M. Steger, K. West, L. N. Pfeiffer, D. W. Snoke, J. Levinsen, M. M. Parish, A. G. Truscott, and E. A. Ostrovskaya, Observation of quantum depletion in a nonequilibrium exciton–polariton condensate, Nat. Commun. **11**, 429 (2020).

[17] D. D. Solnyshkov, H. Terças, K. Dini, and G. Malpuech, Hybrid Boltzmann–Gross-Pitaevskii theory of Bose-Einstein

condensation and superfluidity in open driven-dissipative systems, Phys. Rev. A **89**, 033626 (2014).

[18] M. Kulczykowski and M. Matuszewski, Phase ordering kinetics of a nonequilibrium exciton-polariton condensate, Phys. Rev. B **95**, 075306 (2017).

[19] H. Haug and A.-P. Jauho, *Quantum Kinetics in Transport and Optics of Semiconductors*, 2nd ed., Springer Series in Solid-State Sciences (Springer-Verlag, Berlin Heidelberg, 2008).

[20] L. P. Kadanoff and G. Baym, *Quantum Statistical Mechanics* (Westview Press, Cambridge, Mass, 1962).

[21] T. R. Kirkpatrick and J. R. Dorfman, Transport in a dilute but condensed nonideal Bose gas: Kinetic equations, J. Low. Temp. Phys. **58**, 301 (1985).

[22] H. Haug, T. D. Doan, and D. B. Tran Thoai, Structure formation, superfluid velocity patterns, and induced vortex-antivortex oscillations and rotations in microcavity polaritons, Phys. Rev. B **91**, 195311 (2015).

[23] S. Utsunomiya, L. Tian, G. Roumpos, C. W. Lai, N. Kumada, T. Fujisawa, M. Kuwata-Gonokami, A. Löffler, S. Höfling, A. Forchel, and Y. Yamamoto, Observation of Bogoliubov excitations in exciton-polariton condensates, Nat. Phys. **4**, 700 (2008).

[24] T. Horikiri, T. Byrnes, K. Kusudo, N. Ishida, Y. Matsuo, Y. Shikano, A. Löffler, S. Höfling, A. Forchel, and Y. Yamamoto, Highly excited exciton-polariton condensates, Phys. Rev. B **95**, 245122 (2017).

[25] T. Byrnes, T. Horikiri, N. Ishida, M. Fraser, and Y. Yamamoto, Negative Bogoliubov dispersion in exciton-polariton condensates, Phys. Rev. B **85**, 075130 (2012).

[26] H. Haug and H. H. Kranz, Bose-Einstein condensation in nonequilibrium systems, Z. Phys. B: Condensed Matter **53**, 151 (1983).

[27] H. Haug and S. Schmitt-Rink, Electron theory of the optical properties of laser-excited semiconductors, Prog. Quantum Electron. **9**, 3 (1984).

[28] M. Aßmann, J.-S. Tempel, F. Veit, M. Bayer, A. Rahimi-Iman, A. Löffler, S. Höfling, S. Reitzenstein, L. Worschech, and A. Forchel, From polariton condensates to highly photonic quantum degenerate states of bosonic matter, Proc. Natl. Acad. Sci. USA **108**, 1804 (2011).

[29] G. Margolin and K. Smolarkiewicz, Antidiffusive velocities for multipass donor cell advection, SIAM J. Sci. Comput. **20**, 907 (1989).

[30] Y. Sun, P. Wen, Y. Yoon, G. Liu, M. Steger, L. N. Pfeiffer, K. West, D. W. Snoke, and K. A. Nelson, Bose-Einstein Condensation of Long-Lifetime Polaritons in Thermal Equilibrium, Phys. Rev. Lett. **118**, 016602 (2017).

[31] N. M. Hugenholtz and D. Pines, Ground-state energy and excitation spectrum of a system of interacting Bosons, Phys. Rev. **116**, 489 (1959).